Eur. Phys. J. A (2020) 56:103
https://doi.org/10.1140/epja/s10050-020-00081-4

THE EUROPEAN PHYSICAL JOURNAL A

Regular Article -Theoretical Physics

Multiplicity dependence of strange and multi-strange hadrons in p–p, p–Pb and Pb–Pb collisions at LHC energies using Tsallis–Weibull formalism

Pritam Chakraborty[1], **Tulika Tripathy**[1], **Subhadip Pal**[2], **Sadhana Dash**[1,a]

[1] Indian Institute of Technology Bombay, Powai, Mumbai 400076, India
[2] Indian Institute of Science Education and Research Kolkata, Mohanpur 741246, India

Received: 16 October 2019 / Accepted: 31 January 2020 / Published online: 3 April 2020

Communicated by Tamas Biro

Abstract The transverse momentum (p_T) distribution of strange hadrons (K^0_S and Λ) and multi-strange hadrons(Ξ and Ω) measured in p–p, p–Pb, and Pb–Pb collisions at LHC energies has been studied for different multiplicity classes using Tsallis–Weibull (or q-Weibull) formalism. The distribution describes the measured p_T spectra for all multiplicity (or centrality) classes. The multiplicity dependence of the extracted parameters were studied for the mentioned collision systems. The λ parameter was observed to increase systematically with the collision multiplicity and follows a mass hierarchy for all collision systems. This characteristic feature indicates that λ can be associated to the strength of collectivity in heavy ion collisions. It can also be related to strength of dynamic effects such as multi-partonic interactions and color reconnections which mimic collectivity in smaller systems. The non-extensive q parameter is found to be greater than one for all the particles suggesting that the strange particles are emitted from a source which is not fully equilibrated.

1 Introduction

The study of collisions of relativistic heavy ions at RHIC and LHC energies allows us to understand the formation of the new phase of matter created at extreme conditions of temperature and density. The key observables studied in heavy ion collisions to characterize the produced system are often studied in smaller collision systems such as proton-nucleus (p–A) and elementary proton-proton (p–p) collisions to disentangle the effects of initial and final stages of the collision. The recent observations in high multiplicity p–p and p–Pb collisions at LHC energies such as the enhanced production of strange particles [1–3], the long-range correlations ("ridge" structure) in the near-side region of the two-particle correlations [4,5], hardening of spectra of identified particles which become more pronounced for massive particles [3] and few more are reminiscent of creation of a deconfined medium as produced in A–A collisions.

One of the proposed signatures of the formation of this novel state is the enhanced production of strange and multi-strange hadrons [6]. The strange quarks are predominantly produced in the parton-parton scattering processes (like flavor creation and flavor excitation) as they are not present in the initial state of colliding nuclei. The abundance of strange partons in the deconfined medium results in the production of more strange particles compared to p–p collisions [6,7]. The yield of strange particles in central and mid-central collisions has been well described by statistical hadronization models assuming a grand canonical ensemble approach [8]. However, in smaller systems like p–p collisions, the relative abundance of strange hadrons is reduced compared to A–A collisions. This observation was attributed to the effects of canonical suppression which imposes a local conservation of strangeness quantum number in a canonical ensemble formalism while producing strange hadrons [9]. However, this mechanism does not explain the strangeness production in peripheral collisions at RHIC where a smaller system was expected to be produced [10]. The system produced in p–A collisions can be considered to be intermediate between the heavy-ion and the p–p collisions in terms of particle multiplicity and volume of the system. Therefore, the study and comparison of particle production in these systems is crucial in order to interpret the effects of canonical formalism and hadronization in general. The recent observation of strangeness enhancement in high multiplicity p–Pb and p–p collisions indicated towards the progressive lifting of canonical suppression with increase in particle multiplicity [2,3].

[a] e-mail: Sadhana.Dash@cern.ch (corresponding author)

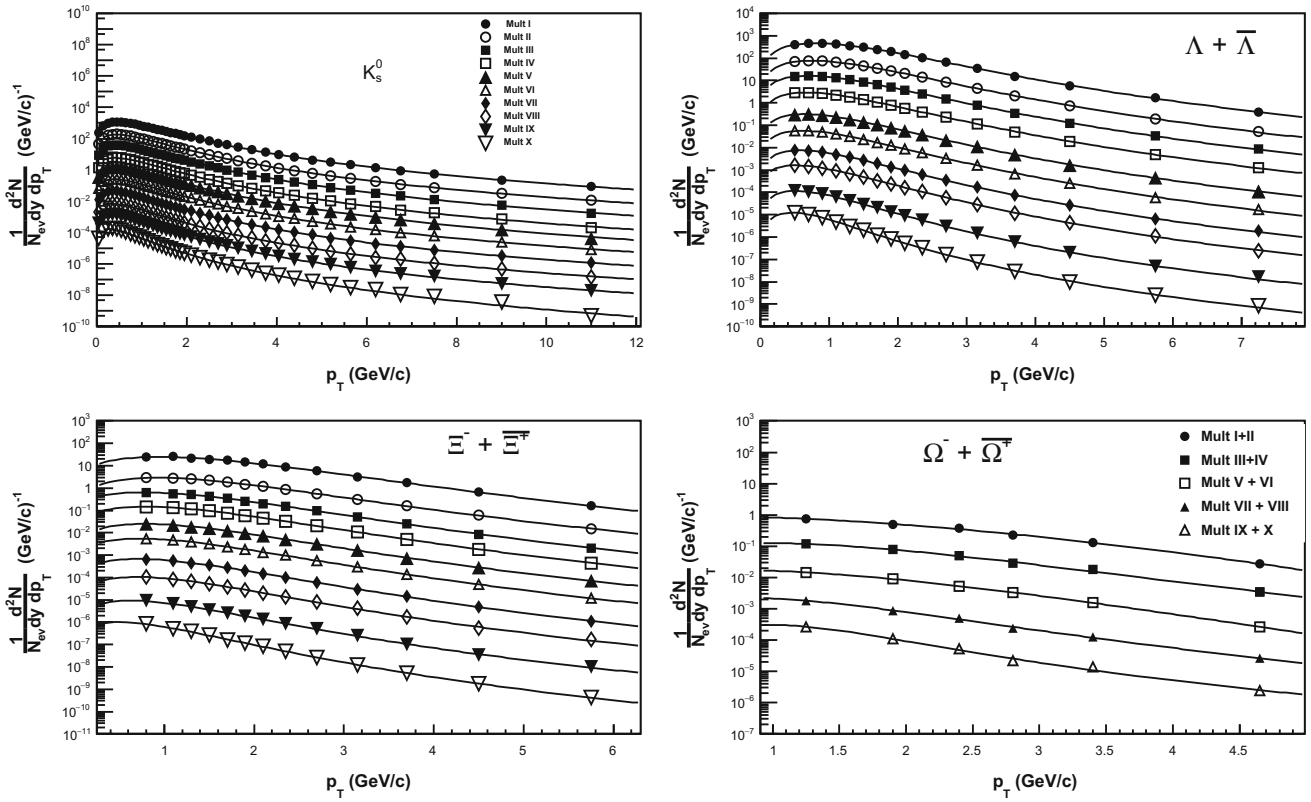

Fig. 1 p_T distribution of strange and multi-strange hadrons in p–p collisions at $\sqrt{s} = 7$ TeV for $|\eta| < 0.8$ as measured by ALICE experiment at LHC [3]. The solid lines are the q-Weibull fits to the data points. The data points are properly scaled for visibility

Therefore, it is worth investigating the transverse momentum (p_T) distribution of the produced strange hadrons created in such collisions within different statistical frameworks, to understand the strange particle production, as the integrated effects of dynamics of particle production from initial stages of collision leaves its footprints in the p_T spectra. The particle production in high energy collisions is usually divided into soft and hard production regimes. The low p_T regime is dominated by soft hadron production and the p_T spectra of the produced particles can be described by Boltzmann–Gibbs statistics. The high p_T region is well described by a power law type of distribution as the hadrons are produced by hard-scattering processes dominant in the initial stages. Generally, the Tsallis statistical distribution is used to describe data for elementary p–p collisions over a wide range of p_T because of its two limits: the power law like shape at large p_T and exponential distribution at small p_T. The flow parameter is introduced is Tsallis distribution to explain the hadronic spectra in heavy ion collisions to account for the effects of collectivity [11–14]. A recent work/study also explained the p_T spectra in high energy collisions using the Pareto–Hagedron–Tsallis distribution which emphasized the application of non-extensive statistics in describing particle production features in high energy collisions [15]. The intermittency studies has

Table 1 The values of $\langle dN_{ch}/d\eta \rangle_{\eta<0.5}$ for different multiplicity classes for p–p collisions at $\sqrt{s} = 7$ TeV [1]

Multiplicity class	$\langle dN_{ch}/d\eta \rangle$	Multiplicity class	$\langle dN_{ch}/d\eta \rangle$
I	21.5 ± 0.6	VI	8.45 ± 0.25
II	16.5 ± 0.5	VII	6.72 ± 0.21
III	13.5 ± 0.4	VIII	5.40 ± 0.17
IV	11.5 ± 0.3	IX	3.90 ± 0.14
V	10.1 ± 0.3	X	2.26 ± 0.12

shown about the multi-fractal aspects in the dynamics behind particle production. The non-extensive Tsallis statistics have been associated to thermofractal structures, and to conjectured fractal structures in Yang-Mills Fields [16,17]. A previous has shown that the Tsallis–Weibull (or q-Weibull) distribution described the p_T spectra of charged particles in p–p, p–A and A–A collisions for the measured p_T range [18]. In this work, the Tsallis–Weibull (q-Weibull) distribution has been used to describe the p_T distribution in classes of multiplicity for strange and multi-strange hadron production in p–p, p–Pb and Pb–Pb collisions at LHC energies. The parameters which characterize the distribution have been studied as a function of charged particle density and centrality to

understand their evolution with collisions dynamics. This study allows to extend the q-Weibull formalism to identified strange particles in order to gain a clear physical interpretation of the associated parameters.

2 The q-Weibull distribution

The natural evolving processes where the dynamic evolution is governed by fragmentation and sequential branching are described by Weibull distribution [19,20]. The production of hadrons in non-perturbative domain has an inherent cascade branching fragmentation and therefore Weibull distribution successfully described the multiplicity distribution of charged particles in hadron-hadron and leptonic collisions [21,22]. The Weibull-distribution is incorporated with Tsallis statistics to obtain q-Weibull distribution.

Mathematically, the q-Weibull distribution is obtained by replacing the exponential factor in Weibull distribution by its equivalent q-exponential [23,24].

$$P_q(x;q,\lambda,k) = \frac{k}{\lambda}\left(\frac{x}{\lambda}\right)^{k-1} e_q^{-(\frac{x}{\lambda})^k} \tag{1}$$

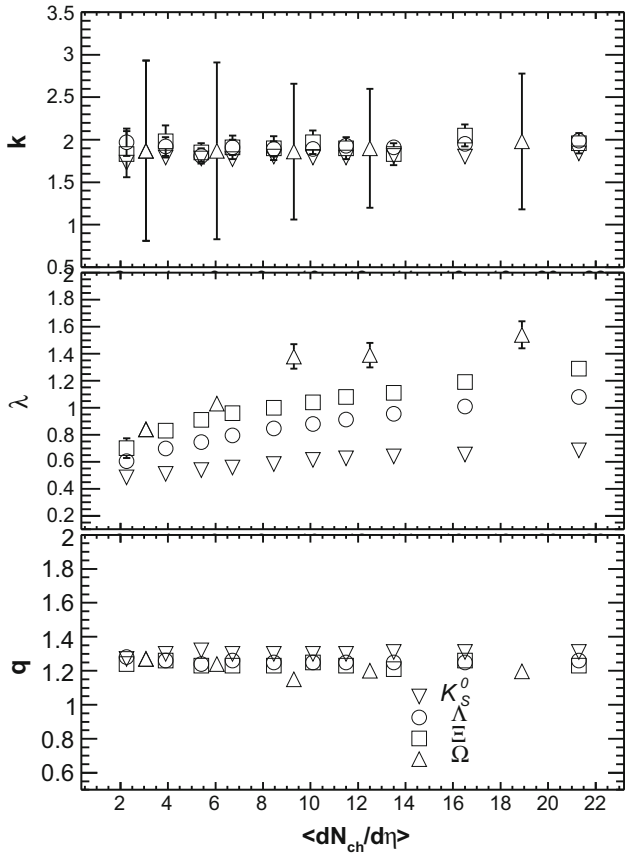

Fig. 2 Variation of k (upper panel), λ (middle panel) and q (lower panel) as a function of $\langle dN_{ch}/d\eta\rangle$ for p–p collisions at $\sqrt{s} = 7$ TeV

Table 2 The values of k, λ, q and χ^2/ndf obtained from the fits of p_T distributions using q-Weibull function in p–p collisions at $\sqrt{s} = 7$ TeV for different multiplicity classes as measured by ALICE experiment at LHC [1,3]

$\langle dN_{ch}/d\eta\rangle$	k	λ	q	χ^2/ndf
K^0_S				
21.3 ± 0.6	1.84 ± 0.02	0.68 ± 0.007	1.31 ± 0.005	0.8
16.5 ± 0.5	1.80 ± 0.02	0.65 ± 0.007	1.31 ± 0.005	0.54
13.5 ± 0.4	1.81 ± 0.02	0.64 ± 0.006	1.31 ± 0.004	1.3
11.5 ± 0.3	1.79 ± 0.02	0.62 ± 0.006	1.30 ± 0.004	1.65
10.1 ± 0.3	1.79 ± 0.02	0.61 ± 0.006	1.30 ± 0.004	2.03
8.45 ± 0.25	1.80 ± 0.02	0.58 ± 0.005	1.30 ± 0.004	1.09
6.72 ± 0.21	1.77 ± 0.02	0.55 ± 0.005	1.30 ± 0.004	0.69
5.40 ± 0.17	1.78 ± 0.02	0.54 ± 0.001	1.32 ± 0.001	1.7
3.90 ± 0.14	1.79 ± 0.02	0.51 ± 0.005	1.30 ± 0.005	0.9
2.26 ± 0.12	1.73 ± 0.03	0.48 ± 0.006	1.27 ± 0.005	2.13
$\Lambda + \overline{\Lambda}$				
21.3 ± 0.6	1.99 ± 0.08	1.082 ± 0.02	1.26 ± 0.02	0.18
16.5 ± 0.5	1.95 ± 0.08	1.00 ± 0.018	1.25 ± 0.02	0.15
13.5 ± 0.4	1.91 ± 0.08	0.95 ± 0.017	1.25 ± 0.02	0.10
11.5 ± 0.3	1.93 ± 0.08	0.91 ± 0.017	1.25 ± 0.02	0.14
10.1 ± 0.3	1.89 ± 0.08	0.88 ± 0.017	1.25 ± 0.02	0.16
8.45 ± 0.25	1.89 ± 0.09	0.85 ± 0.016	1.25 ± 0.02	0.24
6.72 ± 0.21	1.91 ± 0.09	0.79 ± 0.016	1.26 ± 0.02	0.17
5.40 ± 0.17	1.81 ± 0.09	0.75 ± 0.003	1.24 ± 0.02	1.56
3.90 ± 0.14	1.92 ± 0.11	0.70 ± 0.02	1.26 ± 0.02	0.40
2.26 ± 0.12	1.97 ± 0.16	0.60 ± 0.03	1.28 ± 0.02	0.430
$\Xi^- + \overline{\Xi^+}$				
21.3 ± 0.6	1.96 ± 0.12	1.29 ± 0.03	1.23 ± 0.03	0.74
16.5 ± 0.5	2.05 ± 0.13	1.19 ± 0.02	1.26 ± 0.03	0.38
13.5 ± 0.4	1.83 ± 0.13	1.11 ± 0.02	1.21 ± 0.03	0.53
11.5 ± 0.3	1.90 ± 0.13	1.08 ± 0.02	1.23 ± 0.03	0.17
10.1 ± 0.3	1.97 ± 0.14	1.04 ± 0.03	1.25 ± 0.03	0.16
8.45 ± 0.25	1.89 ± 0.14	1.0 ± 0.02	1.23 ± 0.03	0.35
6.72 ± 0.21	1.91 ± 0.14	0.96 ± 0.03	1.23 ± 0.03	0.39
5.40 ± 0.17	1.85 ± 0.11	0.91 ± 0.02	1.23 ± 0.03	1.10
3.90 ± 0.14	1.97 ± 0.19	0.83 ± 0.04	1.26 ± 0.03	0.68
2.26 ± 0.12	1.83 ± 0.27	0.70 ± 0.07	1.24 ± 0.04	0.34
$\Omega^- + \overline{\Omega^+}$				
18.9 ± 0.6	1.98 ± 0.8	1.54 ± 0.1	1.196 ± 0.03	0.74
12.5 ± 0.5	1.90 ± 0.7	1.38 ± 0.09	1.2 ± 0.03	0.38
9.3 ± 0.4	1.86 ± 0.8	1.37 ± 0.09	1.15 ± 0.03	0.53
6.06 ± 0.3	1.87 ± 0.13	1.03 ± 0.01	1.24 ± 0.03	0.17
3.08 ± 0.3	1.87 ± 0.14	0.84 ± 0.026	1.27 ± 0.03	0.16

where

$$e_q^{-(\frac{x}{\lambda})^k} = \left(1 - (1-q)\left(\frac{x}{\lambda}\right)^k\right)^{\left(\frac{1}{1-q}\right)} \tag{2}$$

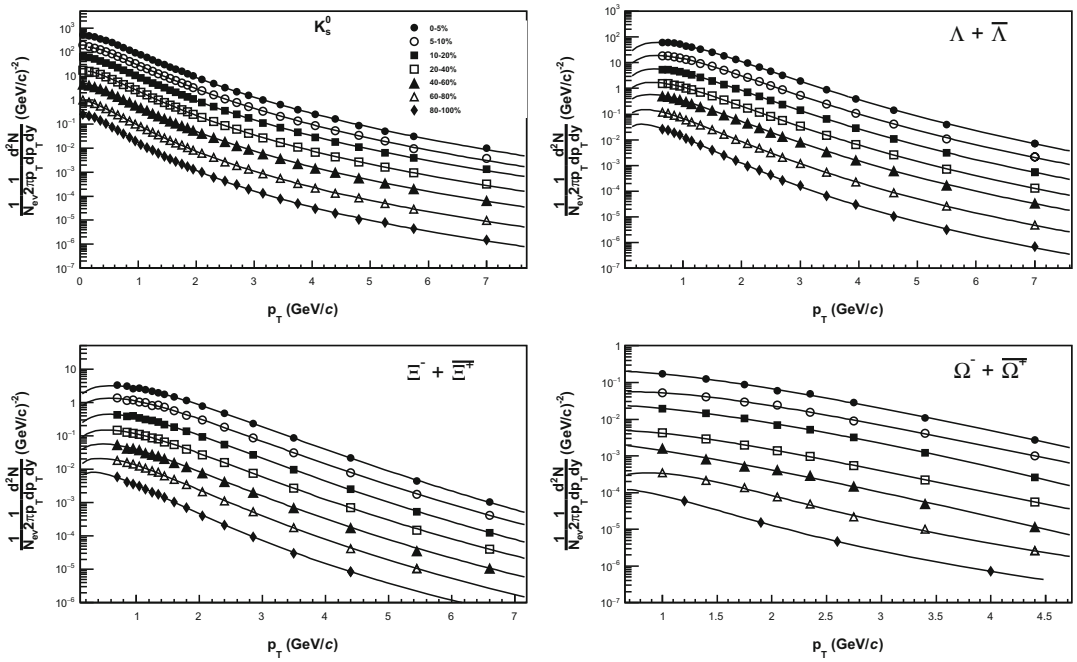

Fig. 3 p_T distribution of strange and multi-strange hadrons in different multiplicity classes for p–Pb collisions at 5.02 TeV for $|\eta| < 0.8$ as measured by ALICE experiment at LHC [2,25]. The solid lines are the q-Weibull fits to the data points. The data points are properly scaled for visibility

As observed in previous analysis of p_T spectra of charged particles in heavy ion collisions [18], the value of the non-extensive q parameter is related to the deviation of the system from thermal equilibrium. In general, $q > 1$ value is attributed to the presence of intrinsic fluctuations in the system and depends upon the observable being measured. The λ parameter can be associated with the mean p_T in hadronic collisions or the collective expansion velocity of hadrons in heavy ion collisions. The k parameter can be related to system dynamics associated with the type of collisions.

3 Analysis and discussion

In a previous study [18], the q-Weibull distribution was successful in explaining the p_T distribution of charged particles in p–p, p–A, A–A collisions for the measured p_T range for most of the beam energies studied. In this work, the analysis has been extended to identified strange and multi-strange hadrons in these collision systems. The p_T distribution of strange and multi-strange hadrons in different multiplicity classes were fitted with q-Weibull function in p–p [3], p–Pb [2,25],and Pb–Pb [26,27] collisions at beam energies of 7 TeV, 5.02 TeV, and 2.76 TeV, respectively as measured by ALICE experiment. The fitting is performed on basis of χ^2 minimization procedure using ROOT libraries and the systematic studies were done by varying the fitting ranges.

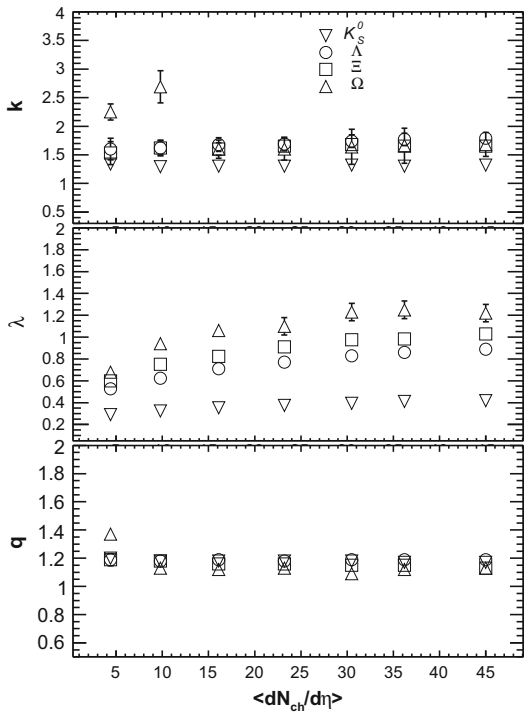

Fig. 4 Variation of k (upper panel), λ (middle panel) and q (lower panel) as a function of $\langle dN_{ch}/d\eta \rangle$ for p–Pb collisions at $\sqrt{s} = 5.02$ TeV

Figure 1 shows the invariant yield of K^0_S, Λ^0, $\Xi^{\pm}$ and $\Omega^{\pm}$ as a function of p_T for p–p collisions at $\sqrt{s} = 7$ TeV for ten different multiplicity classes. The definition of multi-

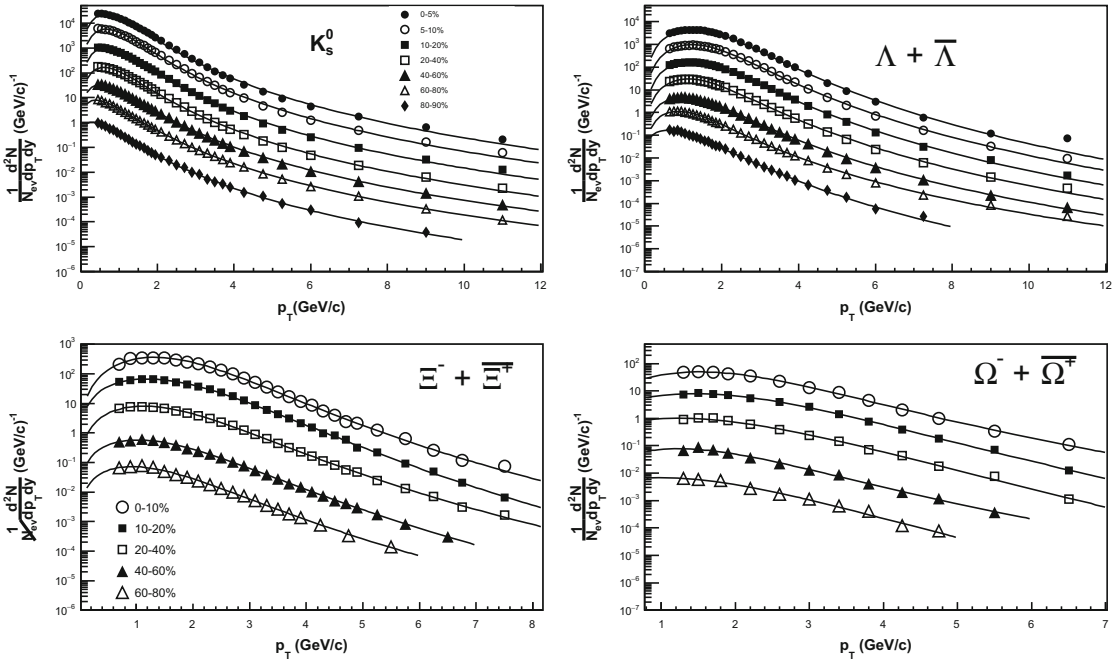

Fig. 5 p_T distribution of strange and multi-strange hadrons for various centrality classes in Pb–Pb collisions at $\sqrt{s_{NN}} = 2.76$ TeV for $|\eta| < 0.8$ as measured by ALICE experiment at LHC [26,27]. The solid lines are the q-Weibull fits to the data points. The data points are properly scaled for visibility

plicity classes and the associated values of $\langle dN_{ch}/d\eta \rangle_{\eta<0.5}$ based on measurement by ALICE experiment [1] is shown in Table 1. The spectra is observed to be nicely described by q-Weibull function for all multiplicity classes as shown by solid lines in the figure. The evolution of values of the extracted fit parameters with respect to the mean charged particle density ($\langle dN_{ch}/d\eta \rangle$) corresponding to different multiplicity classes is shown in Fig. 2. The values of the extracted fit parameters together with the χ^2/ndf are shown in Table 2. The q parameter is observed to be greater than one for the measured strange and multi-strange hadrons for all multiplicity classes. These values are consistent with the non-equilibrium scenario present in p–p collisions. The λ parameter which is related to the mean p_T shows a gradual decrease from higher multiplicity classes to lower ones. It can also be noted that the values are higher for massive hadrons compared to the lesser massive ones. This observation seems interesting and is reminiscent of the onset of collective motion as observed in heavy ion collisions. However, other mechanisms like increase of multi-partonic interactions and color reconnections in final stages as predicted by fragmentation models [28–30] can play an important role in this observation. The k value which was predicted to be related to the dynamical processes contributing to non-equilibrium scenario (dominant in initial stages) [18] is almost independent of multiplicity and the values are similar for the selected hadrons within uncertainties.

Figure 3 shows the description of p_T spectra for strange and multi-strange hadrons in p–Pb collisions at 5.02 TeV [2,25] for different multiplicity classes. The variation of q-Weibull parameters as a function of $\langle dN_{ch}/d\eta \rangle$ is shown in Fig. 4. The p_T distribution of K^0_S, Λ^0, $\Xi^{\pm}$ and $\Omega^{\pm}$ in Pb–Pb collisions at 2.76 TeV [26] in different centrality classes is shown in Fig 5. Figure 6 shows the centrality (N_{part}, number of participating nucleons in a collision) dependence of parameters for different strange hadrons. Tables 3 and 4 shows the value of the extracted parameters for identified strange particles in p–Pb and Pb–Pb collisions, respectively. As can be observed from the figures, q-Weibull fits provide an excellent description of the data for both the collision systems for a broad range of centrality classes. The λ values show a systematic increase from peripheral to central collisions for all the studied strange hadrons. The values are also consistently higher for massive hadrons compared to the lesser ones in both the systems. This observation is consistent with the presence of collective motion (as per transverse expansion scenario in hydrodynamic evolution) in heavy ion collisions which increases with centrality. An increase in collective radial flow implies an increase in mean p_T and the presence of collective radial flow creates a mass ordering of mean p_T. The λ parameter exhibits both behaviors and thus λ can be related to collective velocity of particles and therefore to mean p_T. The same behavior is seen in p–Pb collisions, which is interesting and suggests the presence of collective effects in p–Pb collisions. The parameter k shows a slight decrease as we move from central to peripheral collisions in both Pb–Pb while it is not evident nor significant

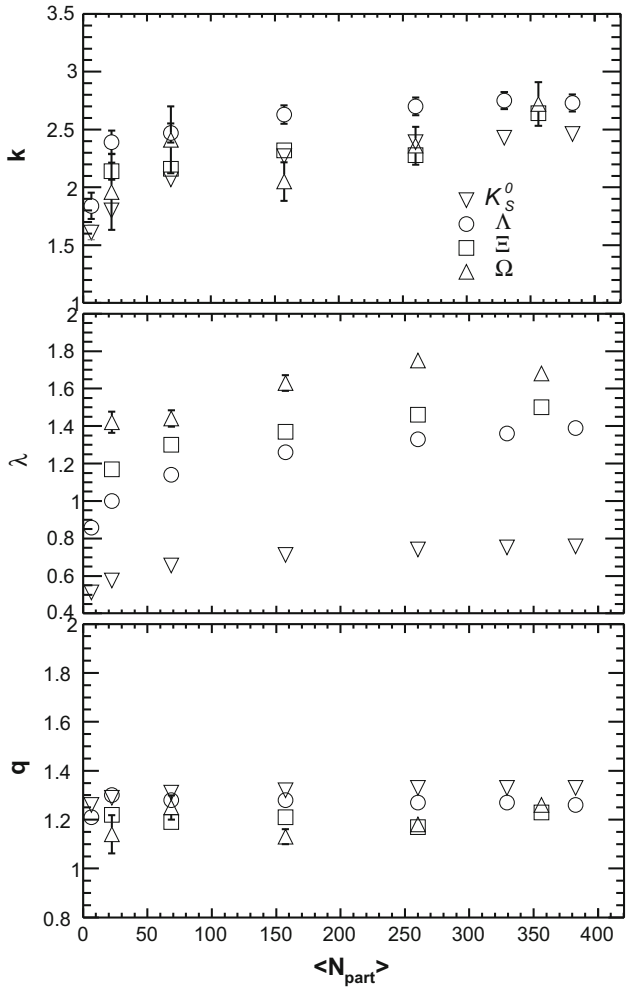

Fig. 6 Variation of k (upper panel), λ (middle panel) and q (lower panel) as a function of $\langle N_{part} \rangle$ for Pb–Pb collisions at $\sqrt{s_{NN}} = 2.76$ TeV

in p–Pb collisions within the uncertainties. This indicates that the value of k parameter increases with onset of processes leading to non-equilibrium conditions. The deviation from local equilibrium can be quantified by the non-extensive parameter, q. The q values show a deviation from one which decreases slightly from central to peripheral collisions. A detailed investigation of other identified particles in terms of system size and beam energies is required to obtain a clear and consistent interpretation of the parameters.

4 Summary

The study of production of strange and multi-strange particles in different systems have become quite relevant with the recent observation of strangeness enhancement in high multiplicity p–p collisions at LHC energies. The q-Weibull statistics has been applied for the first time to comprehend the p_T distribution of strange and multi-strange hadrons in different colliding systems (p–p , p–Pb and Pb–Pb) for a broad range of multiplicity classes. The q-Weibull function successfully describes the p_T distribution for all ranges of p_T measured. The evolution of the parameters of the distribution extracted from the fit were studied as a function of multiplicity for all the collision systems. The λ parameter which was conjectured to be associated with the collective expansion velocity was observed to systematically increase with the collision centrality in Pb–Pb and p–Pb collisions.

Table 3 The values of k, λ, q and χ^2/ndf obtained from the fits of p_T distributions using q-Weibull function in p–Pb collisions for different multiplicity classes at $\sqrt{s_{NN}} = 5.02$ TeV as measured by ALICE experiment at LHC [2,25]

Multiplicity percentile (%)	$\langle dN_{ch}/d\eta \rangle$	k	λ	q	χ^2/ndf
K^0_S					
0–5	45 ± 1	1.32 ± 0.03	0.42 ± 0.01	1.17 ± 0.01	0.4
5–10	36.2 ± 0.8	1.30 ± 0.03	0.41 ± 0.01	1.17 ± 0.01	0.5
10–20	30.5 ± 0.7	1.32 ± 0.03	0.39 ± 0.01	1.18 ± 0.01	0.3
20–40	23.2 ± 0.5	1.3 ± 0.03	0.37 ± 0.01	1.18 ± 0.01	0.2
40–60	16.1 ± 0.4	1.3 ± 0.03	0.35 ± 0.01	1.18 ± 0.01	0.1
60–80	9.8 ± 0.2	1.29 ± 0.03	0.32 ± 0.01	1.18 ± 0.01	0.1
80–100	4.4 ± 0.1	1.34 ± 0.04	0.29 ± 0.01	1.20 ± 0.01	0.3
$\Lambda + \overline{\Lambda}$					
0–5	45 ± 1	1.79 ± 0.10	0.88 ± 0.03	1.19 ± 0.02	0.1
5–10	36.2 ± 0.8	1.77 ± 0.11	0.86 ± 0.03	1.25 ± 0.02	0.1
10–20	30.5 ± 0.7	1.74 ± 0.11	0.83 ± 0.03	1.25 ± 0.02	0.05
20–40	23.2 ± 0.5	1.69 ± 0.12	0.77 ± 0.03	1.25 ± 0.02	0.05
40–60	16.1 ± 0.4	1.68 ± 0.12	0.71 ± 0.03	1.25 ± 0.02	0.1
60–80	9.8 ± 0.2	1.62 ± 0.14	0.62 ± 0.04	1.25 ± 0.03	0.1
80–100	4.4 ± 0.1	1.60 ± 0.19	0.52 ± 0.03	1.26 ± 0.03	0.2
$\Xi^- + \overline{\Xi^+}$					
0–5	45 ± 1	1.65 ± 0.09	1.03 ± 0.03	1.13 ± 0.02	0.3
5–10	36.2 ± 0.8	1.65 ± 0.09	0.98 ± 0.03	1.15 ± 0.02	0.5
10–20	30.5 ± 0.7	1.68 ± 0.09	0.97 ± 0.02	1.15 ± 0.02	0.2
20–40	23.2 ± 0.5	1.65 ± 0.09	0.91 ± 0.02	1.16 ± 0.02	0.1
40–60	16.1 ± 0.4	1.60 ± 0.11	0.82 ± 0.03	1.16 ± 0.02	0.3
60–80	9.8 ± 0.2	1.62 ± 0.12	0.75 ± 0.03	1.18 ± 0.02	0.1
80–100	4.4 ± 0.1	1.53 ± 0.2	0.59 ± 0.05	1.19 ± 0.04	0.2
$\Omega^- + \overline{\Omega^+}$					
0–5	45 ± 1	1.68 ± 0.2	1.22 ± 0.08	1.13 ± 0.03	0.6
5–10	36.2 ± 0.8	1.66 ± 0.3	1.25 ± 0.08	1.12 ± 0.03	0.4
10–20	30.5 ± 0.7	1.64 ± 0.3	1.23 ± 0.08	1.09 ± 0.03	0.2
20–40	23.2 ± 0.5	1.60 ± 0.1	1.1 ± 0.08	1.13 ± 0.03	0.1
40–60	16.1 ± 0.4	1.60 ± 0.1	1.06 ± 0.03	1.12 ± 0.03	1.6
60–80	9.8 ± 0.2	2.69 ± 0.7	0.94 ± 0.03	1.13 ± 0.03	0.5
80–100	4.4 ± 0.1	2.25 ± 0.1	0.68 ± 0.03	1.37 ± 0.03	0.16

Table 4 The values of k, λ, q and χ^2/ndf obtained from the fits of p_T distributions using q-Weibull function in Pb–Pb collisions for different centrality classes at $\sqrt{s_{NN}} = 2.76$ TeV as measured by ALICE experiment at LHC [26,27]

Centrality (%)	$\langle N_{part} \rangle$	k	λ	q	χ^2/ndf
K^0_S					
0–5	382.7 ± 3.0	2.46 ± 0.05	0.76 ± 0.01	1.33 ± 0.01	1.8
5–10	329.4 ± 4.3	2.43 ± 0.05	0.75 ± 0.01	1.32 ± 0.01	1.5
10–20	260.1 ± 3.8	2.39 ± 0.05	0.74 ± 0.01	1.32 ± 0.01	2.1
20–40	157.2 ± 3.1	2.27 ± 0.05	0.71 ± 0.01	1.32 ± 0.01	1.2
40–60	68.6 ± 2.0	2.07 ± 0.05	0.66 ± 0.01	1.30 ± 0.01	1.1
60–80	22.3 ± 0.8	1.80 ± 0.05	0.57 ± 0.01	1.28 ± 0.01	0.5
80–90	6.4 ± 4.2	1.61 ± 0.06	0.51 ± 0.01	1.26 ± 0.01	1.3
$\Lambda + \overline{\Lambda}$					
0–5	382.7 ± 3.0	2.73 ± 0.07	1.39 ± 0.02	1.26 ± 0.01	1.2
5–10	329.4 ± 4.3	2.75 ± 0.07	1.36 ± 0.02	1.27 ± 0.02	1.3
10–20	260.1 ± 3.8	2.70 ± 0.08	1.33 ± 0.02	1.27 ± 0.02	1.1
20–40	157.2 ± 3.1	2.63 ± 0.08	1.26 ± 0.02	1.28 ± 0.02	1.1
40–60	68.6 ± 2.0	2.47 ± 0.08	1.14 ± 0.02	1.28 ± 0.02	0.5
60–80	22.3 ± 0.8	2.39 ± 0.09	1.00 ± 0.02	1.30 ± 0.02	0.9
80–90	6.4 ± 4.2	1.84 ± 0.13	0.85 ± 0.03	1.21 ± 0.02	0.1
$\Xi^- + \overline{\Xi^-}$					
0–10	356.1 ± 3.6	2.64 ± 0.05	1.50 ± 0.01	1.22 ± 0.01	1.4
10–20	260.1 ± 3.8	2.28 ± 0.04	1.46 ± 0.01	1.17 ± 0.01	1.8
20–40	157.2 ± 3.1	2.31 ± 0.05	1.37 ± 0.02	1.21 ± 0.01	2.1
40–60	68.6 ± 2.0	2.16 ± 0.05	1.30 ± 0.01	1.19 ± 0.01	0.7
60–80	22.3 ± 0.8	2.13 ± 0.07	1.17 ± 0.01	1.21 ± 0.02	1.6
$\Omega^- + \overline{\Omega^+}$					
0–10	356.1 ± 3.6	2.71 ± 0.18	1.67 ± 0.03	1.25 ± 0.03	1.1
10–20	260.2 ± 3.8	2.36 ± 0.16	1.74 ± 0.03	1.17 ± 0.03	1.2
20–40	157.2 ± 3.1	2.04 ± 0.16	1.62 ± 0.04	1.12 ± 0.03	1.3
40–60	68.9 ± 2.0	2.41 ± 0.28	1.43 ± 0.04	1.24 ± 0.04	2.1
60–80	22.3 ± 0.8	1.95 ± 0.32	1.41 ± 0.06	1.13 ± 0.05	2.6

A mass hierarchy was also observed i.e. the particles with higher mass had larger values of λ. These features are consistent with the presence of collectivity(radial flow) in the medium formed and hence one can attribute λ parameter to the collective velocity. A similar behavior for the variation of λ with multiplicity was also observed for p–p collisions. For p–p collisions, this parameter can be related to strength of other mechanisms like multi-partonic interactions and color reconnections which mimic features of collectivity. The q parameter which is related to the degree of deviation from conditions of thermal equilibrium was almost a constant with respect to centrality for all collision systems studied. The values consistently deviated from one for all the collision systems and were also higher for Pb–Pb and p–Pb collisions indicating that the system from which the strange hadrons are emitted is not fully equilibrated. The values of k show a slight variation with centrality where the values decrease while moving from higher multiplicity to lower ones for certain particles. It can be related to certain dynamical features of collision which indicate the presence of processes which are dominant in initial stages of collision.

Acknowledgements The authors would like to thank the Department of Science and Technology (DST), India for supporting the present work.

Data Availability Statement This manuscript has associated data in a data repository. [Authors' comment: The experimental data used in the present manuscript was published by ALICE experiment [2,3,25–27].]

References

1. J. Adams et al. (ALICE Collaboration), Nat. Phys. **13**, 535–539 (2017)
2. B. Abelev et al. (ALICE Collaboration), Phys. Lett. B **758**, 389–401 (2016)
3. S. Acharya et al. (ALICE Collaboration), Phys. Rev. C **99**, 024906 (2019)
4. V. Khachatryan et al. (CMS Collaboration), JHEP **09**, 091 (2010)
5. V. Khachatryan et al. (CMS Collaboration), Phys. Rev. Lett. **116**(17), 172302 (2016)
6. J. Rafelski, B. Muller, Phys. Rev. Lett. **48**, 1066 (1982)
7. P. Koch, B. Muller, J. Rafelski, Phys. Rep. **142**, 167 (1986)
8. P. Braun-Munzinger, K. Redlich, J. Stachel, in *Quark Gluon Plasma 3*, ed. by R.C. Hwa, X.-N. Wang (World Scientific, Singapore, 2004), pp. 491–599
9. K. Redlich, A. Tounsi, Eur. Phys. J. C **24**, 589–594 (2002)
10. G. Agakishiev et al. (STAR Collaboration), Phys. Rev. Lett. **108**, 072301 (2012)
11. J. Cleymans, G.I. Lykasov, A.S. Parvan, A.S. Sorin, O.V. Teryaev, D. Worku, Phys. Lett. B **723**, 351–354 (2013)
12. G. Wilk, Z. Wlodarczyk, Phys. Rev. Lett. **84**, 2770 (2000)
13. K. Saraswat, P. Shulka, V. Kumar, V. Singh, Eur. Phys. J. A **53**, 84 (2017)
14. A. Khuntia, S. Tripathy, R. Sahoo, J. Cleymans, Eur. Phys. J. A **53**(5), 103 (2017)
15. K.-M. Shen, J. Phys. G Nucl. Part. Phys. **46**, 105101 (2019)
16. A. Deppman, Phys. Rev. D **93**, 054001 (2016)
17. A. Deppman, E. Megias, D. Perez Menezes, (2019). arXiv:1905.06382
18. S. Dash, D.P. Mahapatra, Eur. Phys. J. A **54**, 55 (2018)
19. W.K. Brown, K.H. Wohletz, J. Appl. Phys. **78**, 2758 (1995)
20. W.K. Brown, J. Astrophys. Astron. **10**, 89–112 (1989)
21. S. Dash, B.K. Nandi, P. Sett, Phys. Rev. D **93**, 114022 (2016)
22. S. Dash, B.K. Nandi, P. Sett, Phys. Rev. D **94**, 074044 (2016)
23. S. Picoli Jr., R.S. Mendes, L.C. Malacarne, Phys. A **324**, 678–688 (2003)
24. S. Picoli Jr., R.S. Mendes, L.C. Malacarne, R.P.B. Santos, Braz. J. Phys. **39**(2A), 468–474 (2009)
25. B. Abelev et al. (ALICE Collaboration), Phys. Lett. B **728**, 25–38 (2014)
26. B. Abelev et al. (ALICE Collaboration), Phys. Lett. B **728**, 216–227 (2014)
27. B. Abelev et al. (ALICE Collaboration), Phys. Rev. Lett. **111**, 222301 (2013)
28. C. Flensburg, G. Gustafson, L. Lonnblad, JHEP **08**, 103 (2011)
29. Christian Bierlich, Jesper Roy Christiansen, Phys. Rev. D **92**, 094010 (2015)

30. T. Sjostrand, S. 'Ask, J.R. Christiansen, R. Corke, N. Desai, P. Ilten, S. Mrenna, S. Prestel, C.O. Rasmussen, P.Z. Skands, Comput. Phys. Commun. **191**, 159–177 (2015)
31. B. Abelev et al. (ALICE Collaboration), Phys. Rev. C **88**, 044909 (2013)